Theoretical study based on 2D assumptions of the influence of small pores on crack initiation in adhesively bonded joints

N. Carrere, Aurélien Doitrand, E. Martin, D. Leguillon

Theoretical study based on 2D assumptions of the influence of small pores on crack initiation in adhesively bonded joints

N. Carrere[1]*, A. Doitrand[2], E. Martin[3], D. Leguillon[4]

1 IRDL, CNRS 6027, Brest, France
* corresponding author nicolas.carrere@ensta-bretagne.fr
2 MATEIS, CNRS UMR 5510, Villeurbanne F-69621 Cedex, France
3 LCTS, CNRS UMR 5801, Université Bordeaux, Pessac, France
4 IJLRA, CNRS UMR 7190, Université P. et M. Curie, Paris, France

---

Abstract

The intrinsic performance of epoxy adhesives seems to designate them as the ideal solution for assembling certain materials. Pore can have an influence on the load at which the first crack is initiated and on the final strength. In the context of damage tolerance, this work aims to explore the effect of small voids that cannot be detected by conventional non-destructive testing (NDT). To attain this goal, a method based on a criterion coupling strength and toughness is used. 2D finite-element calculations are performed on simple configurations to understand the steps leading to failure when pores are present. When the defects are far from the edges, the loss in load at the initiation of the first crack is a function of the minimum distance between two pores. When the location of the defect interacts

with the stress concentration due to a free edge, this loss is a function of the minimum spacing between pores and the free edge. The knock-down factor on the load at failure for a bonded joint with epoxy adhesives remains small (close to the defect area divided by the total area of the bondline). The presence of pores may change the fracture surface (from an adhesive one without pore to a cohesive one with pores).

Keywords: Finite-element stress analysis, Fracture mechanics, Epoxides, Defect

1. Introduction

Adhesively bonded joints represent a very interesting alternative to mechanical joints especially for composite structures. However, for aeronautical applications, its use is still limited due to the difficulty of fulfilling the requirements imposed by certification specifications (see [1]). One of the main challenges is related to the *establishment of a repeatable and reliable non-destructive inspection technique that ensures the strength of each joint*. In order to attain this goal, it is necessary to use Non-Destructive Testing (NDT) capable of detecting defects that could have a significant effect on the failure load. Different forms of NDT exist to control the quality of a joint (for instance ultrasound, radiography, thermography). The comparison of these techniques is out of the scope of this article and a review can be found in the work by *Adams et al.* [2] [3]. However, it is necessary to remind

that these procedures are characterised by the size of the defect they are able to detect, by the ability to determine its position within the thickness of the glue joint and by the size of the specimen that can be inspected. From a design point of view, it must be demonstrated that the structure will be able to resist in the presence of defects larger than a certain threshold (for instance, defined according to the Non-Destructive Testing and the industrial application). Such an approach, termed damage tolerance, requires the development of experiments and models in order to investigate the nature of defects and their effect on the load at failure. Recent results obtained by Dumont *et al.* using X-ray microtomography [4] have highlighted the presence of pores after the manufacturing process. These pores are quasi-spherical with a radius that should be smaller than 20 µm and the typical pore ratio is around 2%-3%. The pores are more or less homogeneously distributed within the adhesive (even when close to a free edge). Post-mortem observations have also demonstrated that cracks could be initiated in the vicinity of these pores [4].

Many experimental studies have been carried out on the influence of artificial defects on the failure load of adhesively bonded single-lap joints. For instance, Heidarpour *et al.* [5] introduced defects of varying sizes and shapes in the middle of the overlap of a single-lap joint (by means of a PVC sheet) at the interface of the substrate or within the adhesive. PTFE films with different volume fractions of pores were introduced by Zhanga *et al.* [6] in the middle section of the

adhesive. The pores are regularly distributed in the overlap length. Karachalios *et al.* [7] introduced circular and rectangular defects (of different sizes) inside the adhesive in the middle of the overlap of a single-lap joint. All these studies, in the case of high-yield-strength substrates, demonstrated a quasi-linear variation of the failure load as a function of the ratio between the flaw area and the total overlap surface (termed below as pore surface ratio and noted vp). It is relevent to note that, in all cases, the defects remain large (compared to the thickness of the adhesive) and are located far from the edges of the single-lap joint. Numerical results have shown that the size, shape and number of pores are key parameters which determine the influence of flaws on the stress field. Elhannania *et al.* evidenced [8] that (i) a defect located near the free edge drastically increases the stresses and (ii) the circular shape of the defect leads to higher stresses. With regard to the effect of defects on the failure load of adhesively bonded joints, most of the research has been carried out using cohesive zone models and focuses on artificial defects such as a strip embedded in the adhesive as proposed by Ribeiro *et al.* in [9] or through the thickness of the adhesive in the work of de Moura *et al.* [10]. The results of these numerical works support certain conclusions obtained experimentally: (i) the pore surface ratio and (ii) the location of the defects in relation to the free edges are key parameters. These studies highlight the importance of estimating a knock-down factor associated with pores that takes into account all the key parameters (i.e. pore surface ratio, shape,

distance from the edge) when using a damage tolerance approach. This is the purpose of this work.

It seems difficult to attain this goal using only experimental results. Indeed, manufacturing bonded assemblies with controlled porosities (in terms of volume fraction and position) is an issue and there is no such result in the literature (to the authors' knowledge). This is why, in this work, a theoretical study based on the modelling of the pores associated with a fracture criterion has been chosen. The objective is neither to propose a tool able to model a bonded structure with a realistic description of the microstructure of the pores nor to be exhaustive in terms of adhesives (properties and thickness) or substrates (properties and geometry). The aim is rather to understand in a number of selected (but common) cases the influence of pores on the failure of bonded assemblies in order to guide the choice of non-destructive testing and the associated damage tolerance approach. In order to attain this goal, a criterion coupling strength and fracture toughness proposed by Leguillon [11] will be used. This approach enables a criterion to be established for the initiation of the failure in many engineering problems when a stress concentration is involved, as shown in the review by Weißgraeber *et al.* [12]. The coupled criterion will be presented in Section 2 of this paper. It requires finite-element calculations to be performed in order to compute the stress and the energy conditions. In this work, 2D finite-element calculations with plain-strain assumptions have been carried out. Even if choosing

2D modeling for the pore in the glue joint may reduce the accuracy of the result, this hypothesis does not have an adverse effect here because the objective is to estimate knock-down factors by comparing different configurations with one another (other parameters remaining constant). A comparison with 3D calculations will be performed on one case in order to estimate the influence of the 2D assumption. In order to establish in which cases pores could lead to a significative loss in the initiation and the failure loads, two cases of increasing complexity will be studied. The first one, presented in the third section, concerns the influence of pores located far from the edge. Various simple configurations will be studied in order to investigate the effect of pores on the initiation and failure loads. Elementary failure scenarios caused by the presence of pores will be evidenced. In an actual bonded joint with pores, the failure scenario would be a combination of these elementary scenarios. The second case, presented in the fourth section, concerns the effect of pores located near a stress concentration. The case of a single-lap joint is analyzed. The objective in this section is to investigate the loss in load at initiation and in the failure load due to the presence of pores near the free edge of the bondline. The fifth section will be devoted to a discussion concerning the different configurations that have been studied and the associated elementary scenarios. The last section presents the conclusion.

2. Background on the coupled criterion to study the initiation of a crack

The coupled criterion (CC) combines a stress criterion and an energy criterion to predict the initiation of a crack of length L^i:

(1) The stress criterion assumes that the stress normal to the path of the final crack must be greater than the strength of the adhesive:

$$\sigma_{nn}(x) \geq \sigma^c \text{ for } \forall x \leq L^i \quad (1)$$

It is relevent to note that other strength criteria involving several components of the stress field could be used if required by the problem to be solved.

(2) The energy criterion stipulates that the change of energy between the state without a crack and the state with the crack is equal to 0 under imposed displacement as shown by Li *et al.* in [13] :

$$\Delta W_{\text{pot}} + \Delta W_{\text{crack}} + \Delta W_{\text{diss}} + \Delta W_{\text{kine}} = 0 \quad (2)$$

where ΔW_{pot} is the incremental potential energy of the structure; ΔW_{crack} is the incremental energy consumed by the crack growth, ΔW_{diss} is the energy dissipated by non-elastic behavior and ΔW_{kine} are all the other energies dissipated during the cracking process (kinetic energy for instance). For an imposed displacement, ΔW_{pot} is given by:

$$\Delta W_{\text{pot}} = \frac{1}{2}\int_V \underline{\sigma} : \underline{\epsilon^e} dV \quad (3)$$

where ϵ^e is the elastic strain. The energy consumed by the crack growth is calculated as $\Delta W_{crack} = G^c S(x)$ where G^c is the critical energy release rate and $S(x)$ the surface of the newly created crack ($S(x)$ is defined by the length x of the crack and its width).

For the sake of simplicity, we assume in this section that the adhesive could be described by a linear elastic behavior and $\Delta W_{diss}=0$. Since $\Delta W_{kine} \geq 0$, the energy condition (3) could be written:

$$G_{incr}\left(S\left(L^{i}\right)\right) = -\frac{\Delta W_{pot}}{\Delta S\left(L^{i}\right)} \geq G^{C} \tag{4}$$

where G_{incr} is the incremental rate that is linked to the conventional differential energy release rate by (see the work of Martin *et al.* for instance [14]):

$$G_{incr}(S) = \frac{1}{S}\int_0^S G(A)dA \tag{5}$$

where L^i has been omitted in the expression of S for the sake of simplicity. It can be deduced from (5) that:

$$S\frac{\partial G_{incr}(S)}{\partial S} = G(S) - G_{incr}(S) \tag{6}$$

Equations (1) and (4) must be fulfilled for the smallest possible imposed displacement and for the same length at initiation L^i. In the context of small deformations and linear elasticity assumptions, it is possible to introduce

dimensionless parameters to solve this problem:

$$\begin{cases} \sigma_{nn}(x) = k_{nn}(x)E\dfrac{u}{r_{\mathrm{p}}} \\ G_{incr}\big(S(x)\big) = G_{incr}(x) = A(x)E\dfrac{u^2}{r_p} \end{cases} \tag{7}$$

where u is the applied displacement, and r_p a characteristic dimension of the problem (which will be taken as the pore radius in the next sections) and E the Young's modulus of the material. The dimensionless parameters $k_{nn}(x)$ (termed Normalised *Stress Factor* (*NSF*) below) and $A(x)$ (termed *Normalised Incremental Energy Release Rate* (*NIERR*) below) are a function of the elastic properties (of the adhesive and substrates) and the geometry (thickness of the substrates and adhesive). They are easily evaluated using finite-element calculations in accordance with the procedure explained by Doitrand *et al.* in [15] and are a function of the geometry and the material properties. Classically, near a stress concentration (for instance a hole or defect) the coefficient $A(x)$ is null for $x = 0$ and increases as a function of x, whereas $k_{nn}(x)$ is a decreasing function of x. For a monotonic and increasing applied loading, the increment of crack length L^i at nucleation corresponds to the crack increment for which both conditions (1) and (4) are fulfilled for the same smallest imposed displacement. It is possible to show that L^i is then given by :

$$\frac{A(L^{\,i})}{\left[k_{nn}(L^{\,i})\right]^2} = \frac{L^c}{r_p} \tag{8}$$

where L^c is a characteristic fracture length defined by :

$$L^c = \frac{EG^c}{(\sigma^c)^2} \tag{9}$$

If $\frac{A(x)}{[k_{nn}(x)]^2}$ is a monotonic increasing function of x and is equal to 0 for x = 0, the crack length L^i is obtained by solving (8) and the applied displacement at nucleation u^i is given by :

$$u^i = \begin{cases} \sqrt{\frac{G^c r_p}{A(L^i)E}} \\ \frac{\sigma^c r_p}{k_{nn}(L^i)E} \end{cases} \tag{10}$$

The corresponding applied stress at initiation is given by:

$$\Sigma^i = \frac{\Sigma_{u^a}}{u^a} u^i \tag{11}$$

where u^a is a given applied displacement and Σ_{u^a} is the resulting stress. The stress defined by an uppercase letter (Σ) refers to a macroscopic stress on the assembly. The stress defined by a lowercase letter (σ) refers to a stress in the adhesive.

In more complex cases ($A(x)$ and/or $k_{nn}(x)$ are not monotonic functions of x, the nucleation length and the load at initiation could be determined using an optimisation or numerical approach to solve eq. (7). In this work, a numerical approach, based on a sampling of x, is used to solve eq. (7).

As shown in the review by Weißgraeber *et al.* [12], the CC can be implemented

with the help of matched asymptotic expansions, with full finite-element calculations or analytical solutions (exact or simplified solutions). In this work, finite-element calculations will be used to evaluate the stress and energy.

3. Crack initiation in the vicinity of a pore located far from the edge

Considering a pore located far from the edge, three cases will be studied:

- a single pore inside a joint to investigate the configuration without interaction between pores,
- three pores that can interact to determine the range at which pores interact with each other,

These cases will permit to evidence different evolutions of the NSF and NIERR leading to elementary scenarios for the initiation of a crack from a pore.

The material properties of the adhesive and substrate used in this section are given in Table 1. The thickness of the adhesive is equal to 0.4mm.

Properties	Adhesive	Substrate
Young's modulus (GPa)	1.3	70

Poisson's ratio	0.4	0.3

Table 1: Adhesive and substrate properties

3.1. Effects of material parameters and pore radius: case of an isolated pore in an adhesive joint

This section focuses on the initiation of two symmetric cracks from an isolated pore. The geometry is given in figure 1a. It is close to the geometry used by Dumont *et al.* for in-situ X-ray microtomography tests [4]. The thickness of the joint t_a is equal to 0.4mm and the substrates are square-based section bars (6mm x 6mm). It is assumed that two cracks may initiate from the hole as depicted in figure 1a. In view of the symmetries, only a quarter of the problem is modelled (figure 1b). Finite-element calculations have been performed in order to compute the dimensionless parameters $A(x)$ and $k_{nn}(x)$ (see previous section).

The results are given in figure 2 . The NIERR $A(x)$ is a monotonic increasing function of x. For the larger values of the pore radius r_p ($2r_p > 0.25t_a$), the NSF $k_{nn}(x)$ exhibits a local minimum for $x = x_\sigma^{min}$.

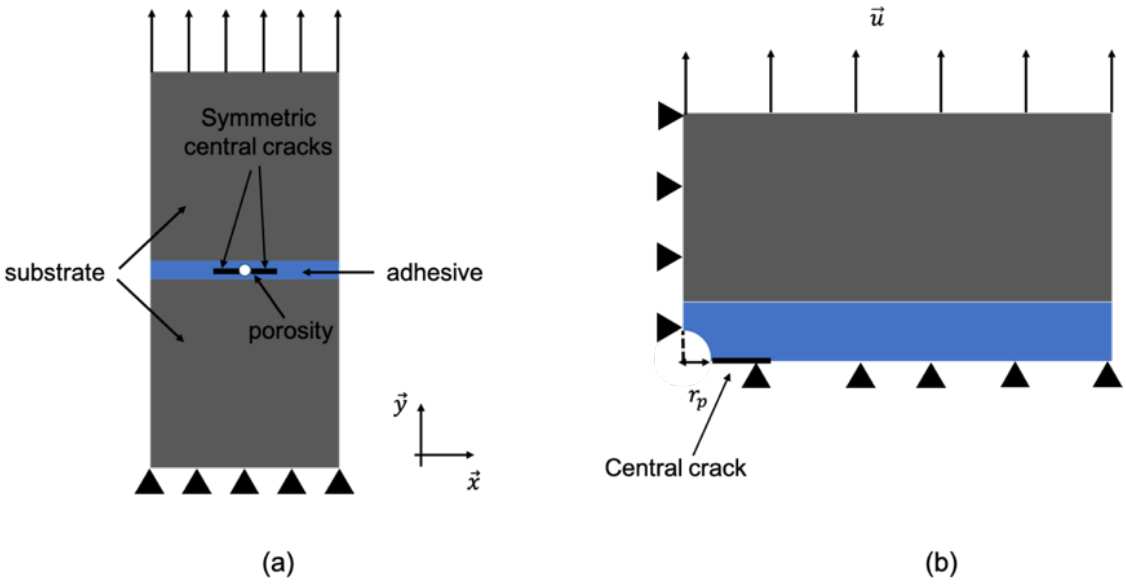

Figure 1 : Global geometry (a) and boundary conditions (isolated pore within the adhesive joint) (b) (not to scale) (thickness of the adhesive 0.4mm, dimension of the bonded surface 6mm*6mm)

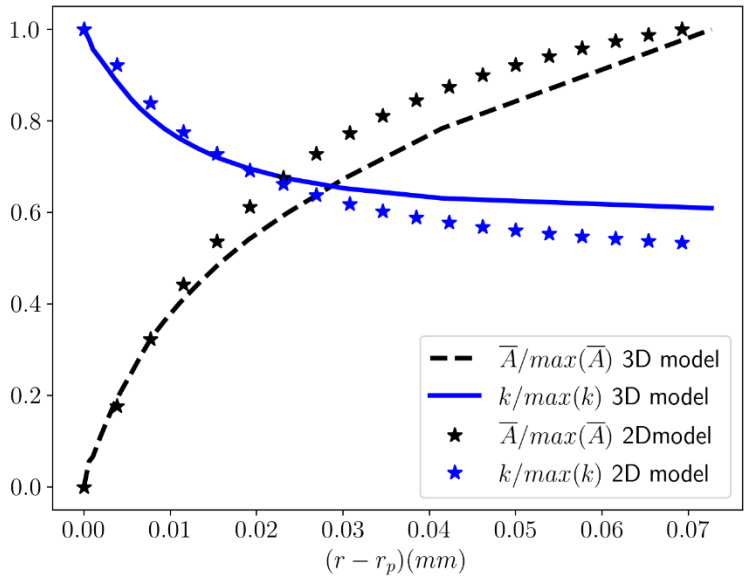

Figure 2 : Dimensionless parameters *A(x)* and $k_{nn}(x)$ (normalised by their maximum value) as a function of r (r=0 is the center of the pore) for an isolated pore with a radius rp equal to 0.04mm (lines: 2D calculations, symbols: 3D calculations)

3D finite-element calculations have been performed in this case to investigate the effect of the 2D assumptions on the calculation of the NIERR and NSF. The application of the coupled criterion for 3D assumptions has been presented by Doitrand *et al.* in [16]. The main difficulty lies in the description of the cracked surface. In order to overcome this issue, the authors proposed to determine the possible crack shapes based on the stress isocontours. The same approach is used in this work. The isovalues have a circular shape centred on the pore. The cracked surface could thus be defined by only one parameter: the radius of the crack.

The comparison of the NIERR $A(x)$ and NSF $k_{nn}(x)$ obtained using 3D or 2D

finite-element calculations is presented in figure 2 . The results obtained using these two assumptions are very similar.

Once the NIERR and NFS are computed, it is possible to determine the length and load at initiation. Two cases could arise:

1. The NSF has no local minimum, or the nucleation length solution of eq. (7) is lower than xσmin. The displacement at nucleation is given by equation (10).

   Moreover, since *Gincr(S(Lᵢ)) = G^c* and Gincr(S(x)) is an increasing function ($\frac{\partial G_{incr}(S)}{\partial S} > 0$), it means that $G_{incr}(\mathrm{S}(x)) \geq G^c \ \forall x \geq L^i$. Thus, once the crack is initiated its propagation is unstable.

2. The NSF has a local minimum, and the nucleation length solution of eq. (7) is greater than xσmin. In this case, the stress condition is fulfilled for ∀ $x \geq x_\sigma^{min}$. The displacement at initiation is governed either by the stress criterion fulfilled at x_σ^{min} or the energetic creation fulfilled where the NIERR is maximum (failure over the total length of the bondline).

These two cases will be labelled in the following as scenario 1: “Initiation of a crack from a pore that does not interact with another pore”.

The nucleation stress Σ^i (nucleation load divided by the bonded surface) normalised by the strength of the joint without pore Σ^{wp} as a function of the

characteristic fracture length for a pore radius of 0.02 mm is given in figure 3 for possible values of L^c for structural epoxy adhesives. For sufficiently high values of the characteristic length L^c (greater than 0.1), the pore has no effect on the nucleation stress. This case corresponds to many structural epoxy adhesives found in the literature : Araldite 2015 L^c=4.98 mm, Araldite AV138 (data from [17]) L^c=0.21 mm and HysolEA9395 L^c=0.26 mm (data from [18]).

For the lower values of the characteristic length (*i.e.* for very brittle adhesive, high strength and/or low toughness), the load at which a crack is initiated from a pore could be less than 10% of the failure load of the joint without pore.

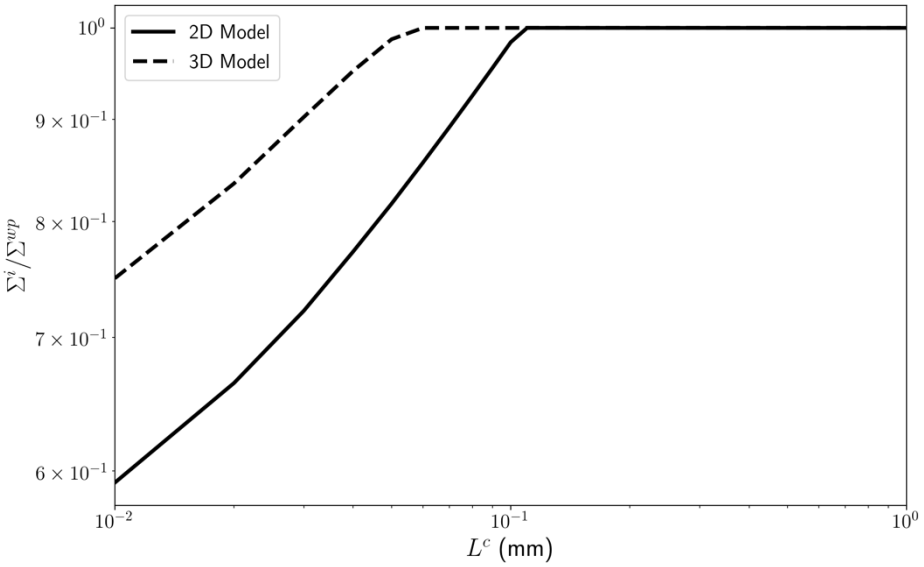

Figure 3: Normalised nucleation stress as a function of the fracture length (L^c) for a pore radius of 0.04 mm with σ^c=25 MPa.

The comparison between the 2D and the 3D assumptions is shown in figure 3. The failure loads differ by at most 25% between the two hypotheses. The 2D assumption leads to conservative results, but the tendencies and the conclusions remain the same.

The variation of the load at which the crack is initiated as a function of the pore radius is given in figure 4 for three sets of fracture properties. These sets of fracture properties have been chosen to cover a representative range of L^c expected in epoxy adhesives. In the case of the greater characteristic length (σ^c = 45*M*Pa, G^c = 0.15N/mm resulting in L^c=0.16mm) the load at initiation is not affected by the pore. For the two other sets of fracture parameters ((σ^c = 45*M*Pa, G^c = 0.1N/mm, L^c=0.06mm) and (σ^c = 60*M*Pa, G^c = 0.25N/mm, L^c=0.09mm)) it is shown that the variation of the nucleation stress as a function of the radius is not monotonic. The case r_p=0.04mm correspond to the one already presented in figure 3. For a small radius, the stress at initiation decreases as a function of the radius. The same trend is observed by Martin *et al.* [19] for an open-hole case (experimental and numerical results based on a finite-fracture approach). For larger pore radii, the load at initiation increases as a function of the radius. This phenomenon could be due to an interaction between the pore and the substrate leading to a stress concentration near the poles of the pore. The same trend is indeed observed by Weißgraeber *et al.* in [20] in the case of an open hole loaded by a concentrated force at the pole of the hole. In the remainder of this section,

the radius of the pore will be chosen in order to avoid any interaction between the pore and the interface (i.e. rp smaller than 0.04mm for an adhesive thickness equal to 0.4mm, i.e. $2r_p/t_a$<0.2).

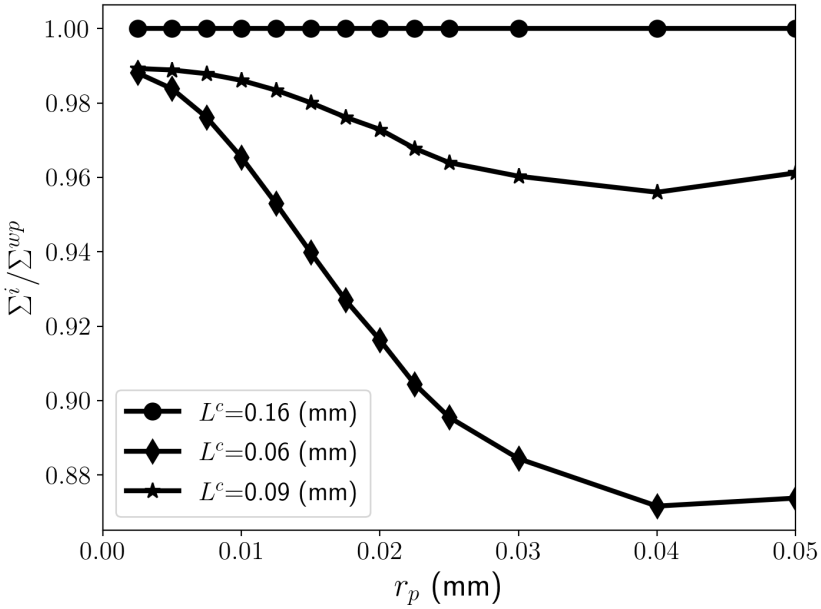

Figure 4: Variation of the normalised nucleation stress as a function of the radius of the pore (adhesive thickness equal to 0.4mm) for three different fracture properties representative of structural epoxy adhesives. The case r_p=0.04mm correspond to the one already presented in figure 3.

These results demonstrate that larger pores do not necessarily result in a higher knock-down factor. Since the objective is to determine whether pores that are barely detectable by NDT have an effect on the load at initiation or at failure, below the size of the pore is chosen equal to 20µm (which is the limit of detection using X-ray tomography in [4]).

3.2. Effects of the distance between two pores: crack initiation when

two pores interact

We will now consider the initiation of two symmetric cracks from a central pore with close neighboring pores (case with only the central crack in figure 5a). In view of these symmetries, only a quarter of the problem is modelled (figure 5b). An example of the variation of the normalised dimensionless parameters is shown in figure 6 for pores with a radius r_p equal to 0.02 mm and a distance between the two pores L of 0.02 mm (the same trend is observed for the other distance between the two pores). It is important to note that the NIERR $A(x)$ is an increasing function of x from the first pore up to the second. It signifies that the maximal initiation length is equal to the distance between the two pores. The NSF $k_{nn}(x)$ exhibits a local minimum for $x = L/2$.

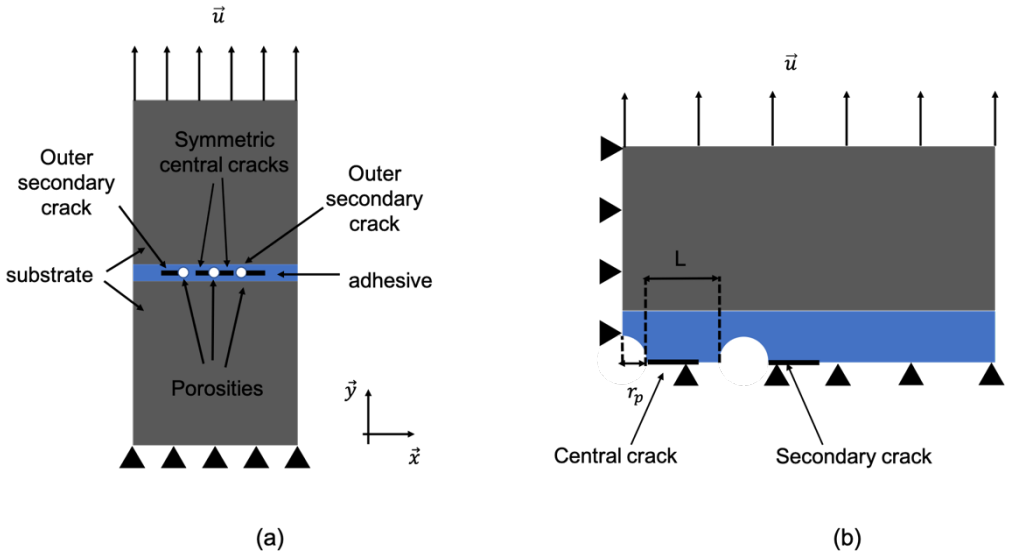

Figure 5: Global geometry (a) and boundary conditions (b) of a central pore with close neighboring pores (thickness of the adhesive 0.4mm, dimension of the bonded surface 6mm*6mm

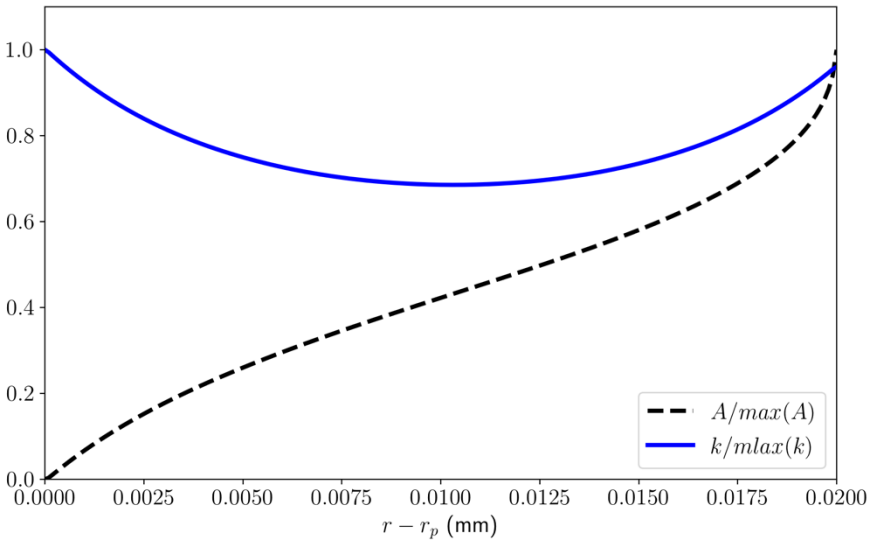

Figure 6: Dimensionless parameters k_{nn}(x) and A(x) (normalized by their maximum value) as a function of r (r=0 is the centre of the first pore) for pores with a radius r_p equal to 0.02mm and a distance between the two pores equal to 0.02mm.

Different cases must be studied and are illustrated in figure 7.

1. The initiation length solution of equation (7) is less than *L/2*. The displacement at nucleation is given by equation (10). The crack is unstable and will propagate after initiation up to *x* = *L*. This case can be classified in the same category as scenario 1.
2. The initiation length solution of equation (7) is greater than or equal to *L/2*. The displacement at initiation is governed either by the stress criterion fulfilled at *L/2* or the energy criterion fulfilled at L:

$$u^i = max\left(\frac{\sigma^c r_p}{k_{nn}(L/2)E}, \sqrt{\frac{G^c r_p}{A(L)E}}\right)$$

If it is the stress criterion that governs, the initiation length is equal to *L/2* and the crack is unstable. If the energy criterion is the governing criterion, the initiation length is equal to *L*. This case will be labelled in the following as scenario 2: “initiation of a crack that interacts with another pore”.

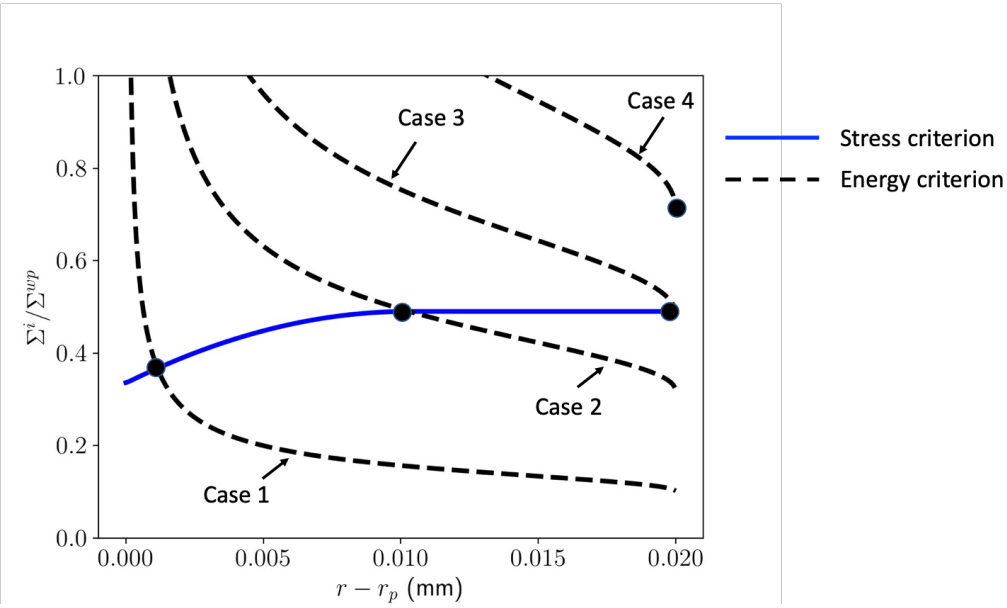

Figure 7: Normalised stress at initiation determined by the stress and energy criterion as a function of *x* for different values of G^c with σ^c = 45 MPa in the case of two pores of radius r_p = 0.02 mm separated by 0.02 mm. The dots are the solutions of the coupled criterion for the different cases. Case 1: G^c leads to an initiation length less than *L*/2. Cases 2 and 3: G^c lead to an initiation length greater than or equal to *L*/2 and the stress criterion is the governing criterion. Case 4: initiation length equal to L and the energy criterion is the governing criterion

The nucleation stress Σ^i (nucleation load divided by the bonded surface) normalised by the strength of the joint without pore Σ^{wp} as a function of the fracture length L^c (possible values for structural epoxy adhesives) for a pore radius of 0.02 mm is given in figure 8. As compared with the previous case (an isolated pore), the nucleation load could be drastically less than the strength of the adhesive if the pores are close enough even for a large value of the fracture parameter.

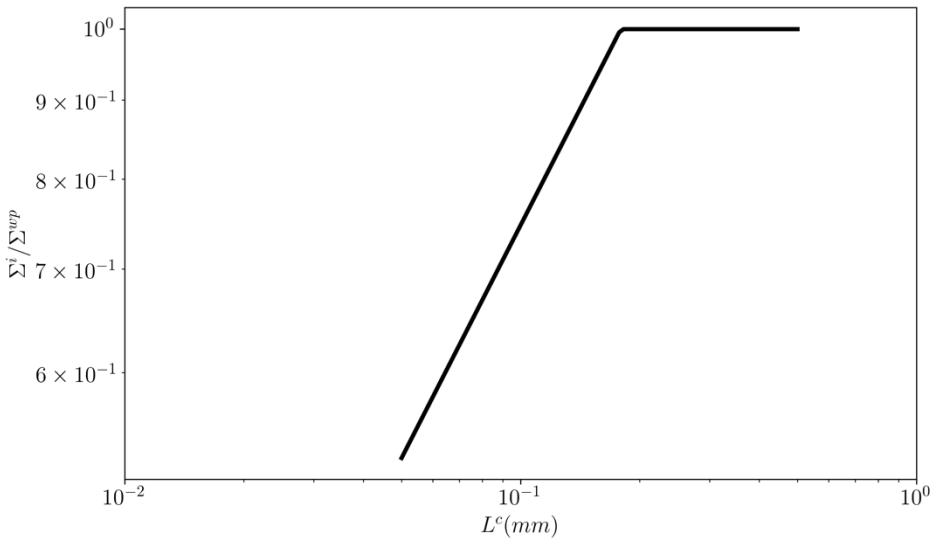

Figure 8: Normalised nucleation stress as a function of the fracture length (L^c) for a pore radius 0.02mm separated by L=0.02 mm with σ^c=25MPa.

The effect of the distance between two pores is shown in figure 9. This figure presents the evolution of the nucleation stress Σ^i (nucleation load divided by the bonded surface) normalised by the strength of the joint with a single pore Σ^{1p}

(with the same radius) as a function of the distance between two pores (*L*). The results show that the closer the pores are, the lower the applied stress at nucleation is. For a greater distance between the two pores, the stress at nucleation tends towards the stress at nucleation obtained with a single isolated pore. This critical distance (that distinguishes the cases where the pores interact or not) is, of course, a function of the fracture length L^c. However, for the sets of fracture parameters investigated, if the distance between two pores is greater than 0.120mm, the stress at nucleation tends towards the stress at nucleation obtained with a single isolated pore.

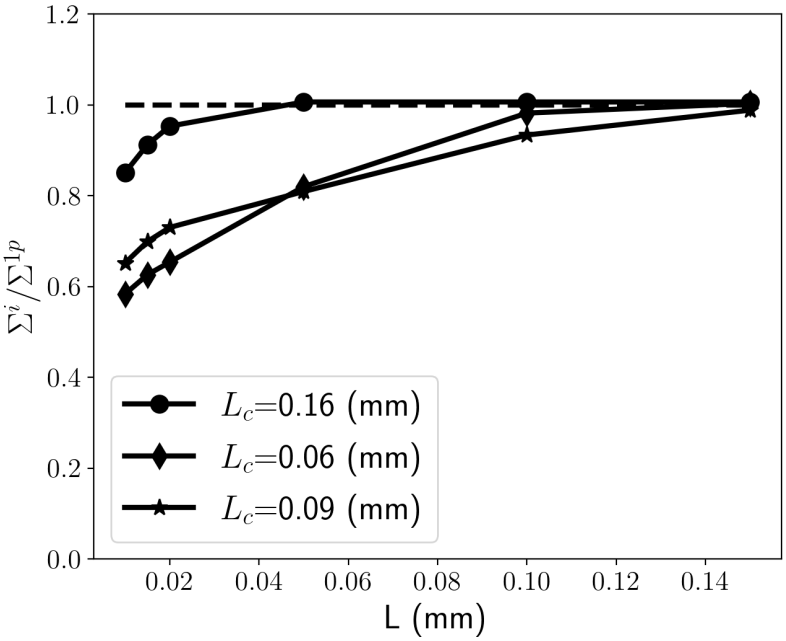

Figure 9: Normalised load necessary to initiate a crack from the central pore as a function the distance L between two pores of radius r_p = 0.02 mm for three different fracture properties representative of structural epoxy adhesives. The dashed line corresponds to the load required to initiate a

crack with a single pore (see Section 3.1).

4. Pores located near the edge of an adhesively bonded joint: case of the single-lap joint

In order to study the effect of pores on the load at initiation and at failure near a stress concentration, the case of the single-lap joint has been chosen (see figure 8). The failure of a single-lap joint has already been studied by the authors using the coupled criterion (work of Moradi *et al.* [23] based on FE calculation or on a semi- analytical approach as proposed by Stein *et al.* in [24]) or a damage model (work of Carrere *et al.* [25]). More information concerning the application of the coupled criterion on single-lap joint is provided in the work of Moradi *et al.* [23] using linear elastic FE calculations (associated with an analytical approach to determine the length and the load at initiation) or in the work of Weißgraeber *et al.* [27] using non-linear elastic FE calculations (associated with an optimisation method to determine the length and the load at initiation). The two methods compared by Weißgraeber *et al.* [26] lead to close results in terms of initiation load (the non-linear analysis leading to a 20% decrease in the failure load for the larger overlap length) but induce different crack paths. The non-linear approach predicts an initiated crack with an angle of 10° whereas this crack is located at the interface for the linear approach. The effect of geometrical non-linearity is not taken into account in this work, but merits investigation in future works. It is

relevent to note that the stress concentration at the free edge is greater in the lower corner than in the upper straight edge. This is why it is assumed below in this case that the failure will occur in the lower corner (as proposed by Moradi *et al.* [23]).

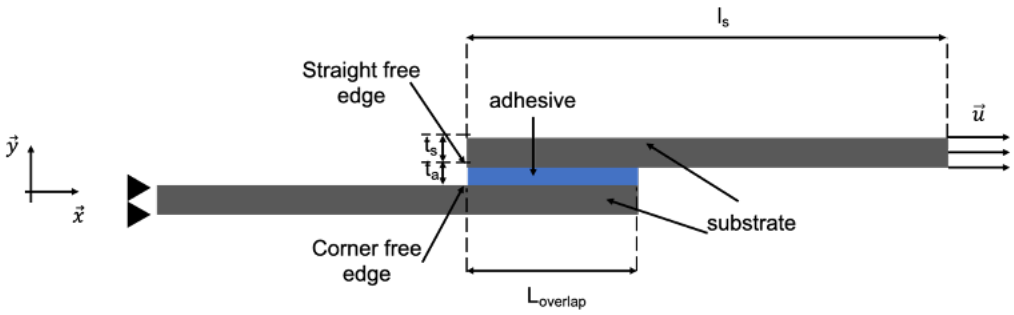

Figure 8: Single-lap joint geometry (not to scale). The specimen width (not visible) is noted w.

The geometry already studied by Da Silva *et al.* [28] is considered as a reference. The substrates are made from high-strength steel (l_s=95 mm, t_s=2 mm, $l_{overlap}$=25 mm, w=25 mm). The adhesive thickness is equal to 0.5 mm. The material properties are given in Table 2. The failure loads reported by Da Silva *et al.* [28] vary between 8.6 kN and 10.2 kN. The application of the coupled criterion results in a load at initiation equal to 9.4 kN and in a crack length at initiation L^i equal to 0.3*mm*. As shown by Carrere *et al.* [25], it is necessary to slightly increase the load to propagate the crack until it reaches a critical length for which the crack

becomes unstable. In this case, the initiation load could be considered as equal to the failure load.

Properties	Adhesive	Substrate
Young's modulus (GPa)	1,3	210
Poisson's ratio	0.4	0.3
Tensile strength (MPa)	46	-
Toughness (N mm−1)	0.5	-

Table 2: Adhesive and substrat properties for single-lap joint cases (from Da Silva *et al.* [28] and Russel [29]

In order to provide some guidance regarding the choice of NDT for an adhesively bonded joint, the objective of this section is to determine which configuration (position of the pores in the joint) will lead to the lowest load at the time of initiation. It is relevent to note that for, the sake of simplicity, the analysis was performed using only the normal out-of-plane stress. A more complete analysis should include a multiaxial state of stress. However, as shown by Carrere *et al.* in [25], for the initiation length obtained in the case investigated here, the mode mix is very close to 1.

An enlargement near the end of the overlap in figure 9a shows the position of the pore in relation to the edge (distance noted d_e) and the interface (d_i). For the same reasons already discussed at the end of Section 3.1, the size of the pore is chosen

to be equal to 20µm (which represents a limit of detection for X-ray tomography and can lead to a significant knock-down factor for the joint thickness under investigation). The crack could be initiated at different locations (figure 9b to d): at the interface or in the plane of the pore (from the pore towards the end of the overlap or from the pore towards the middle of the overlap). It is necessary to study these different cases. The failure mode will be the one resulting in the lower load at initiation.

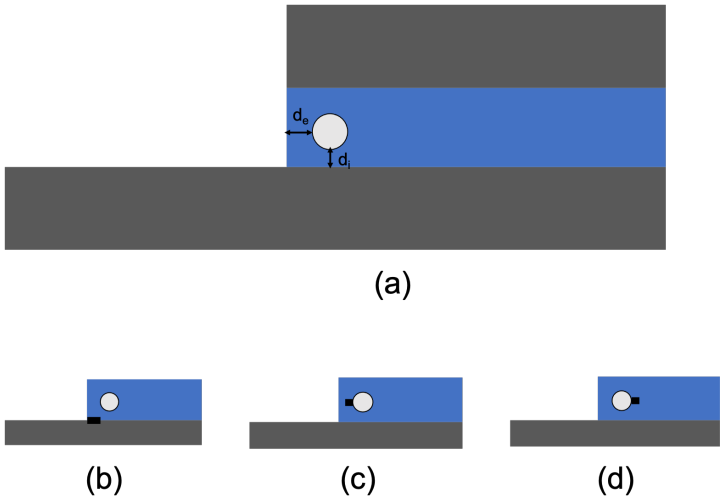

Figure 9: Enlargement near the end of the overlap of a single-lap joint with one pore (not to scale) (a). Possible failure modes: (b) initiation at the interface, (c) initiation from the pore to the edge and (d) initiation from the pore to the middle

Initiation at the interface (figure 9(b)). When a pore is present, the stress at the interface is no longer a monotonic decreasing function (see figure 10). Indeed, the pore tends to locally decrease the stress at the interface as compared with the case without pore (referred to as the reference case below). Far from the

pore, the stress recovers a level equivalent to the reference case. The same trends are observed for the incremental energy release rate. A discussion concerning non-monotonic stress and incremental energy release rate has been proposed by Doitrand *et al.* [30] and will not be reproduced here for the sake of simplicity. Two failure modes are possible: initiation from the free edge or under the pore. In this case (geometry and material properties) the load at which the crack is initiated under the pore is always greater than the other failure mode. This is why it will not be further discussed in this paper. The case where the crack is initiated from the free edge is very similar to the one without pore except if the pore is very close to the interface and the free edge. In this last case, the stress could become locally negative ($\sigma(x) < 0 \ \forall \ x_{neg1} < x < x_{neg2}$). The initiation length is in this case equal to x_{neg1} and the load at initiation is greater than the reference case.

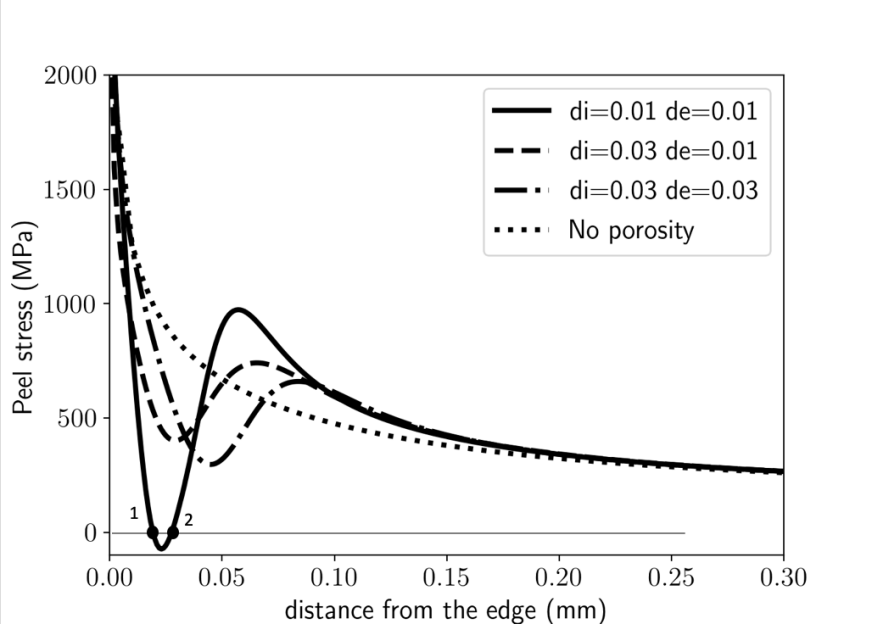

Figure 10: Peel stress along the interface without and with pores (different locations investigated). Point 1 and 2 indicate the location where the stress becomes locally negative for the case *di* = 0.01*mm* and *de* = 0.01*mm*.

Initiation from the pore to the edge (figure 9(c)). The evolution (not shown here for the sake of brevity) of the NSF ($k(x)$) has a local minimum) and the NIERR ($A(x)$ is increasing from the edge to the pore) are the same as that observed in scenario 2. For the fracture properties of the adhesive under investigation, the crack is always initiated over the length corresponding to the distance d_e. Scenario 2 will be extended and designated by "Initiation of a crack from a pore that interacts with another pore or a stress concentration".

Initiation from the pore toward the middle of the overlap (figure 9(d)). In this case, the evolution of the NSF and NIERR (not shown here for reasons of brevity) are similar to the one observed in scenario 1. It is possible to refer to the

discussion associated with this scenario.

The distance from the edges ranges from 0.01mm to 0.3mm, and the distance from the interface from 0.01mm to 0.1mm. The objective is not to study all the possible cases nor to determine the worst one, but to investigate the effect of pores on the load at initiation for chosen pores arrangement.

The load at initiation (S^i_{poro}) normalised by the initiation load without pore (S^i_{wo}) is shown in figure 11. The closer the pore is to the interface and to the edge, the lower the load at initiation. In the worst case investigated in the paper (d_e = 0.01mm and d_i = 0.01mm), the knock-down factor on the load at initiation due to the presence of a pore is greater than 20%. For a pore located far from the interface and edge ($d_e \geq 0.1$mm and $d_i \geq 0.1$mm), the initiation load is equal to the initiation load without pore, and the crack is initiated at the interface between the adhesive and substrate. In the other cases, the crack is initiated from the pore toward the edge (case b).

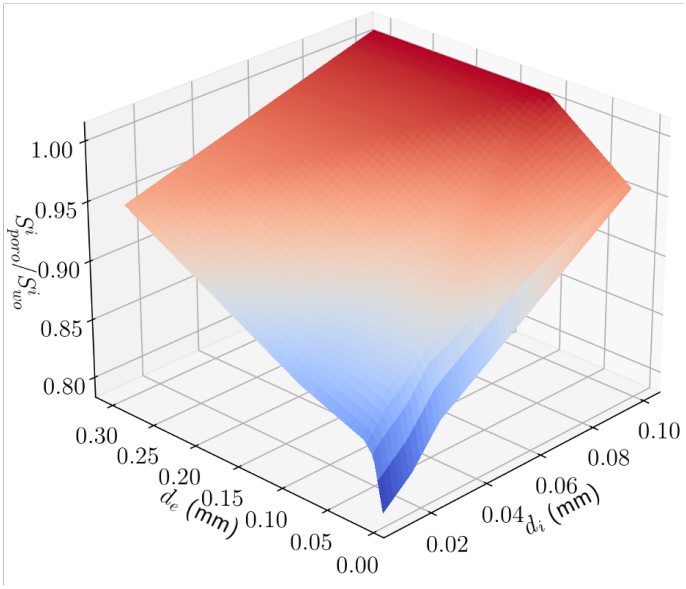

Figure 11 : Normalised initiation load as a function of the location of the pore for a single pore with a radius equal to 20µm (G^c=0.5 N.m-1, σ^c=46MPa)

The last point to investigate concerns the propagation of the crack after initiation. Indeed, it has been shown by Carrere *et al.* [25] for a single-lap joint without pore that once the crack is initiated, a slight increase in the load leads to an unstable propagation and thus total failure. In the presence of pores, even if the load at initiation decreases as compared to the case without pore, it is legitimate to consider whether the crack will propagate in an almost unstable manner.

In order to investigate this case, the same approach presented in Section 3.2 is used. In fact, it is not strictly a crack propagation, but rather a re-initiation of the crack every time that it is stopped by a pore (scenario 2). The case under

investigation corresponds to a row of four pores (see figure 12) with a spacing between two pores corresponding to that of a 2% surface fraction ($\mathrm{L} = \sqrt{\pi r_p^2 / v_p}$) with a first porosity located 10 µ*m* from the edge and 10 µ*m* from the interface (worst case evidenced in figure 11). This is a strong assumption but a horizontal propagation seems likely following the work of Leguillon and Piat [21]. The results presented in figure 12 show that the crack is initiated from the first pore to the edge (for a remote load close to 7.4kN). The propagation of the crack is the result of a jump from one pore to the next. For the three first pores, the re-initiation of the crack requires the load to be increased. The propagation could be seen as stable over a given distance since it requires a significant increase in the remote load (from 7.4kN to 8.6kN) to propagate the crack (unlike in the case without a pore). A strengthening effect due to the presence of the pores, already demonstrated by Leguillon and Piat [21], is thus observed. It is worth mentioning that Leguillon and Piat evidenced that this strengthening effect is a function of the fracture parameters and the geometry (radius of the pore and distance between the pores). Once the crack reaches the third pore, it will jump to the fourth one in an unstable manner. The peak load is considered the failure criterion for the single-lap joint. The same scenario is also observed for different fracture properties representative of structural epoxy adhesives (see figure 13). The peak load is greater than the initiation load, which signifies that the propagation of the

crack is stable over a given length.

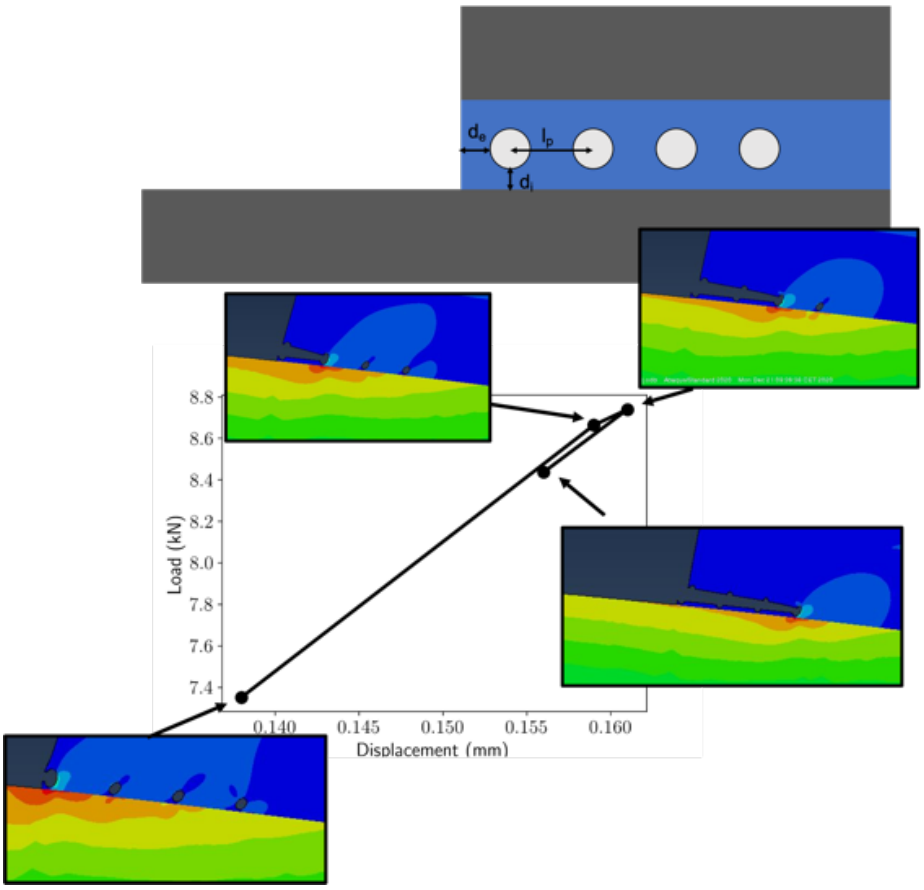

Figure 12: Load vs. displacement curve after crack initiation for a single-lap joint with a row of four pores (radius equal to 20µm, volume fraction of pore equal to 2%, the first pore is located at d_i = 10µm and d_e = 10µm) (G^c=0.5N.m^{-1}, σ^c=46MPa)

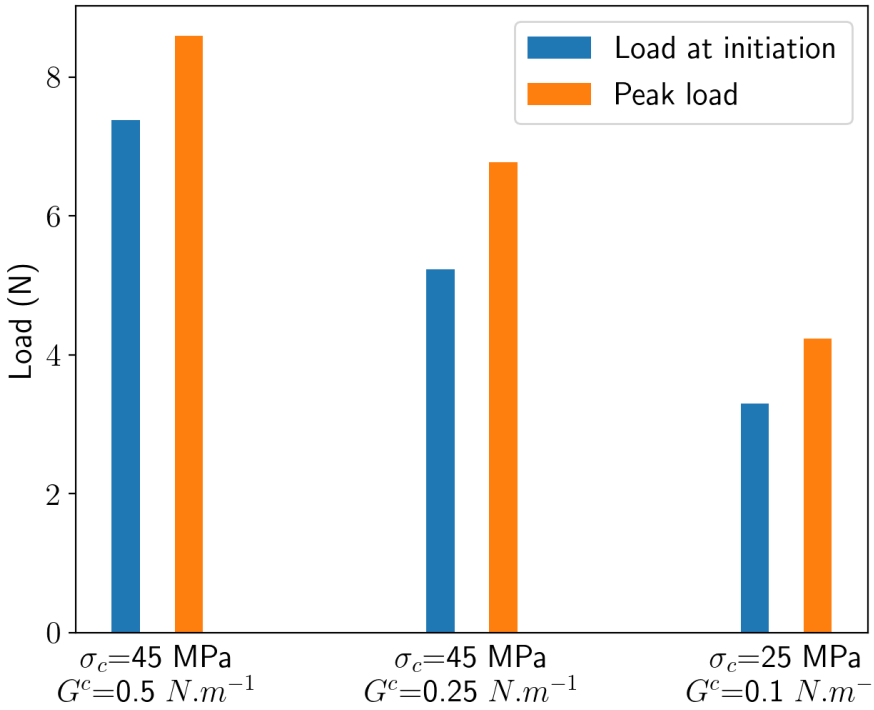

Figure 13: Evolution of the initiation and peak loads for different fracture parameters and the same geometry already plotted in figure 12

5. Discussion

The objective of this section is to provide some guidelines as part of a damage tolerance approach for an adhesively bonded joint with pores. The numerical results obtained in this study show that the effect of pores on the loss of the load at initiation or at failure is a function of (i) the fracture parameters, and (ii) the size, the surface fraction and the location of the pores. Given the objective of this work, its focus is on small porosities in structural exposed adhesives. The effect of fracture parameters representative of structural epoxy adhesives has been

studied. From the experimental works of Zhanga *et al.* [6] and Karachalios *et al.* [7], at first glance, it seems possible to determine an acceptability criterion using the pore volume fraction. However, the results obtained in Section 3.2 also make it possible to conclude that, if locally two pores are close (cluster of pores with a maximum distance of 100µm for conventional epoxy adhesives), the load at the initiation of the crack could be much lower. For an NDT point of view, it signifies that the knowledge of the global pore surface ratio is not sufficient but there is also a need to determine the minimum distance between two pores.

When investigating the fracture mechanisms near a free edge (in the case of a single-lap joint for example) the presence of pores could drastically reduce the load at initiation. Moreover, the presence of the pore could modify the fracture surface from an adhesive fracture without pore to a cohesive fracture with pores (the crack being initiated from the pores). For a conventional epoxy adhesive, the most relevant parameters are the minimum pore/free-edge distance (d_e) and pore/interface distance (d_i). For pores near the edge and near the interface, the load at initiation could be drastically reduced. From an NDT point of view, it signifies that it is also necessary to determine these two distances (d_e) and (d_i).

6. Conclusion

This paper aimed to investigate, from a theoretical point of view, the effect of pores on the load required to initiate a crack in an adhesively bonded joint. An

approach based on modelling the pores associated with a fracture criterion was chosen. Since the aim is to compare different cases to determine the decrease in the failure load due to the pores, in order to reduce the complexity of the model (especially for the single-lap joint configuration), 2D finite-element assumptions were performed. Of particular focus were small pores that are difficult to detect using classical NDT.

Two elementary fracture scenarios were evidenced: (1) “Initiation of a crack from a pore that does not interact with another pore” and (2) “Initiation of a crack from a pore that interacts with another pore or a stress concentration” .

The results demonstrate that even for small pores the load at initiation could be drastically reduced. However, the propagation of the primary crack is not necessarily unstable under monotonic loading. It means that from an NDT point of view, a crack initiated from a pore could be detected during periodic inspection before an unstable failure. From a mechanical point of view, once the crack is initiated it could propagate under cyclic loading, which could lead to a premature failure. The propagation of a crack in an adhesive bond initiated from a pore and interacting with pores remains to be studied.

References

[1] European aviation safety agency, AMC 20-29 Composite Aircraft Structure. https://www.easa.europa.eu/sites/default/files/dfu/Annex%20II%20-

%20AMC%2020-29.pdf

[2] Adams RD, Cawley P, Guyott CCH.. Non-destructive inspection of adhesively-bonded joints. J Adhes. 1987;21 :279–290.

[3] Adams RD,.Cawley P. A review of defect types and non destructive testing techniques for composites and bonded joints. NDT Int 1988;21(4)):208–222.

[4] Dumont V et al. On the influence of mechanical loadings on the porosities of structural epoxy adhesives joints by means of in-situ x-ray microtomography. Int J Adhesion Adhes 2020 ;99

[5] Heidarpour F, Farahani M , Ghabezi P. Experimental investigation of the effects of adhesive defects on the single lap joint strength. Int J Adhesion Adhes 2018;80:128–132.

[6] Zhanga T,Mengd T, Pana Q, Sun B. The influence of adhesive pore on composite joints. Compos Commun 2019;15:87–91.

[7] Karachalios EF, Adams RD, da Silava LFM. Strength of single lap joints with artificial defects. Int J Adhesion Adhes 2013; 45:69–7.

[8] Elhannania M, Madania K, Legrand E , Touzain S ,Feaugas X. Numerical analysis of the effect of the presence, number and shape of bonding defect on the shear stresses distribution in an adhesive layer for the single lap bonded joint; part 1. Aerosp Sci Technol 2017;, 62:122–13.

[9] Ribeiro FMF, Campilho RDSG, Carbas RJC, da Silva LFM. Strength and damage growth in composite bonded joints with defects. Compos Part

B 2016;100:91– 100.

[10] de Moura MFSF, Daniaud R, Magalhaes AG. Simulation of mechanical behaviour of composite bonded joints containing strip defects. Int J Adhesion Adhes 2006;26:464–473.

[11] Leguillon D.. Strength or toughness ? a criterion for crack onset at a notch. Eur J Mech A Solids 2002;21(1):61–7.

[12] Weißgraeber P, Leguillon D, Becker W. A review of Finite Fracture Mechanics: crack initiation at singular and non-singular stress raisers. Arch Appl Mech 2016;86:375-401. https://doi.org/10.1007/s00419-015-1091-7.

[13] Li J, Leguillon D, Martin E, Zhang X-B. Numerical implementation of the coupled criterion for damaged materials. Int J Solids Struct 2019;165:93–103. https://doi.org/10.1016/j.ijsolstr.2019.01.025.

[14] Martin E, Leguillon D. Energetic conditions for interfacial failure in the vicinity of a matrix crack in brittle matrix composites. Int J Solids Struct 2004;41:6937–48. https://doi.org/10.1016/j.ijsolstr.2004.05.044.

[15] Doitrand A, Martin E, Leguillon D. Numerical implementation of the coupled criterion: Matched asymptotic and full finite element approaches. Finite Elements in Analysis and Design 2020;168:103344. https://doi.org/10.1016/j.finel.2019.103344.

[16] Doitrand A, Leguillon D. 3D application of the coupled criterion to crack initiation prediction in epoxy/aluminum specimens under four point bending. J Solids Struct 2018; 143: 175-182

[17] Campilho RDSG. , Banea, MD, Neto JABP, da Silva LFM. Modelling adhesive joints with cohesive zone models: effect of thecohesive law shape of the adhesive layer. Int J Adhesion Adhes 2013;44:48-56.

[18] Ben Salem N, Budzik MK, Jumel J, Shanahan MER, Lavelle F. Investigation of the crack front process zone in the Double Cantilever Beam test with backface strain monitoring technique. Engng Fract Mech 2013:98,2013,272-283.

[19] Martin E, Leguillon D, Carrère N. A coupled strength and toughness criterion for the prediction of the open hole tensile strength of a composite plate. International Journal of Solids and Structures 2012;49:3915–22. https://doi.org/10.1016/j.ijsolstr.2012.08.020.

[20] Weißgraeber P, Hell S, Becker W. Crack nucleation in negative geometries. Engng Fract Mech 2016:168(B):93-104

[21] Leguillon D, Piat R. Fracture of porous materials – Influence of the pore size. Engng Fract Mech 2008;75:1840–53. https://doi.org/10.1016/j.engfracmech.2006.12.002.

[22] Pipes RB, Wetherhold RC, Gillespie JW. Notched strength of composite

materials. J Compos Mater 1979;13:148–60.

[23] Moradi A, Carrère N, Leguillon D, Martin E, Cognard JY. Strength prediction of bonded assemblies using a coupled criterion under elastic assumptions: Effect of material and geometrical parameters. Int J Adhesion Adhes 2013;47:73–82. https://doi.org/10.1016/j.ijadhadh.2013.09.044.

[24]]N.Stein, P.Weißgraeber, W.Becker, A model for brittle failure in adhesive lap joints of arbitrary joint configuration, Compos Struct 2015; 133: 707-718

[25] Carrere N, Martin E, Leguillon D. Comparison between models based on a coupled criterion for the prediction of the failure of adhesively bonded joints. Engng Fract Mech 2015;138:185–2.

[26] Weißgraeber P, Felger J, Talmon l'Armée A, Becker W, Crack initiation in single lap joints: effects of geometrical and material properties. Int J Fract 2015;192:155–166

[27] Weißgraeber P, Becker W. Finite Fracture Mechanics model for mixed mode fracture in adhesive joints. Int J Solids Struct 2013;50:2383–94. https://doi.org/10.1016/j.ijsolstr.2013.03.012.

[28] da Silva LFM, Rodrigues TNSS, Figueiredo MAV, de Moura MFSF,. Chousal JAG. Effect of adhesive type and thickness on the lap shear strength. J Adhesion, 82:1091–1115, 2006.

[29]Russel AJ. A damage tolerance assessement of bonded repairs to cf-18 composite components. part i: Adhesive properties. DREP-Technical Memorandum (88-25), 1988. https://apps.dtic.mil/sti/pdfs/ADA210523.pdf

[30] Doitrand A, Leguillon D. Comparison between 2D and 3D applications of the coupled criterion to crack initiation prediction in scarf adhesive joints. Int J Adhesion Adhes 2018;85:69–76.